Ciliary Body Thickness and Refractive Error in Children

Melissa D. Bailey, Loraine T. Sinnott, and Donald O. Mutti

Purpose. To determine whether ciliary body thickness (CBT) is related to refractive error in school-age children.

Methods. Fifty-three children, 8 to 15 years of age, were recruited. CBT was measured from anterior segment OCT images (Visante; Carl Zeiss Meditec, Inc., Dublin, CA) at 1 (CBT1), 2 (CBT2) and 3 (CBT3) mm posterior to the scleral spur. Cycloplegic refractive error was measured with an autorefractor, and axial length was measured with an optical biometer. Multilevel regression models determined the relationship between CBT measurements and refractive error or axial length. A Bland-Altman analysis was used to assess the between-visit repeatability of the ciliary body measurements.

Results. The between-visits coefficients of repeatability for CBT1, -2, and -3 were 148.04, 165.68, and 110.90, respectively. Thicker measurements at CBT2 ($r = -0.29$, $P = 0.03$) and CBT3 ($r = -0.38$, $P = 0.005$) were associated with increasingly myopic refractive errors (multilevel model: $P < 0.001$). Thicker measurements at CBT2 ($r = 0.40$, $P = 0.003$) and CBT3 ($r = 0.51$, $P < 0.001$) were associated with longer axial lengths (multilevel model: $P < 0.001$).

Conclusions. Thicker ciliary body measurements were associated with myopia and a longer axial length. Future studies should determine whether this relationship is also present in animal models of myopia and determine the temporal relationship between thickening of the ciliary muscle and the onset of myopia. (*Invest Ophthalmol Vis Sci.* 2008;49:4353–4360) DOI:10.1167/iovs.08-2008

Investigators in the Collaborative Longitudinal Evaluation of Ethnicity and Refractive Error (CLEERE) Study have suggested that myopia occurs during two phases of ocular growth: a phase of axial elongation that leads to an increasingly prolate, or less oblate, shape followed by a phase of more uniform global expansion.[1] Other investigators have also reported that the myopic globe is relatively more prolate than the emmetropic globe. In a study using magnetic resonance imaging (MRI) for analysis of globe shape, Atchison et al.[2] reported that the myopic eye is more relatively prolate than the emmetropic eye, with the myopic eye having dimensions that are more elongated axially than in the horizontal or vertical dimensions. Also in 2004, Logan et al.[3] published similar results obtained with A-scan ultrasonography and central and peripheral autorefraction.

A relatively more hyperopic or less myopic peripheral refractive error is a correlate of this relatively prolate shape, particularly in the horizontal meridian, among those with a myopic foveal refractive error.[4–7] There is renewed interest in this classic observation based on both human clinical data and animal experimentation. A longitudinal study of pilots found that relative peripheral hyperopia in an emmetropic eye is associated with an increased risk of development of myopia.[8] Animal experiments also support a potential role for the influence of peripheral input in myopia's development. The retinal periphery is effective in creating axial myopia when deprived of form vision and in directing recovery once normal input is restored.[9] The presence of an intact fovea has been shown to be unnecessary for vision-based alterations to occur in refractive error.[10] As has already been shown for axial hyperopic defocus,[11–14] peripheral hyperopic defocus may contribute to axial elongation and the development of myopia.

A variety of explanations have been proposed to account for the relatively prolate shape of the myopic globe. CLEERE Study investigators have suggested that an internal source of growth restriction might produce the biphasic, increasingly prolate pattern of growth in premyopic eyes, and the crystalline lens has been offered as a potential source of internal growth restriction.[1] Conversely, Atchison et al.[2] suggested an external source of restriction, stating that the differences in axial versus equatorial dimensions were most likely due to the anatomic constraints of the orbital wall.[2] Logan et al.[3] suggested that growth in the axial and transverse dimensions of the globe is regulated differently and independently.[3]

In recent results, Oliveira et al.[15] suggest another possible source of the altered globe shape in myopia. They report an association between refractive error and an ocular component in the equatorial region of the globe; adult patients with myopia were found to have thicker ciliary bodies than those without myopia. The finding that the myopic eye has a thicker rather than thinner ciliary body contradicts the choroidal expansion experiments of van Alphen,[16] who demonstrated marked thinning of the ciliary muscle structure, with little change in the choroid, when the globe was expanded in vitro. Thickening raises the possibility that there is a physiological response of the ciliary body in myopia rather than simple mechanical stretching. Because data from the CLEERE Study,[1] data from Atchison[2] MRI studies, data from Logan et al.,[3] and work in the monkey[9] suggest that the equatorial region of the globe is an important feature in myopia's development, we sought to determine whether the ciliary body is also thicker in myopic children.

Methods

Subjects

Children, 8 to 15 years of age, were recruited by advertisements posted in and around The Ohio State University College of Optometry and letters sent to children who were patients in the Optometry Services. Children with all types of refractive error, but no other ocular diseases, binocular vision abnormalities, or crystalline lens opacities were included. In total, 53 children were recruited for this sample of convenience. This study was conducted in accordance with the tenets of the Declaration of Helsinki. After a presentation and discussion of the procedures and risks associated with the study, all subjects provided written, informed assent, and a parent or legal guardian for each study subject provided written, informed consent. The study procedures and

From The Ohio State University College of Optometry, Columbus, Ohio.

Supported by National Eye Institute Grants K12-EY015447 and R24-EY014792.

Submitted for publication March 11, 2008; revised May 13, 2008; accepted August 25, 2008.

Disclosure: **M.D. Bailey**, None; **L.T. Sinnott**, None; **D.O. Mutti**, None

The publication costs of this article were defrayed in part by page charge payment. This article must therefore be marked "*advertisement*" in accordance with 18 U.S.C. §1734 solely to indicate this fact.

Corresponding author: Melissa D. Bailey, 338 West Tenth Avenue, Columbus, OH 43210; mbailey@optometry.osu.edu.

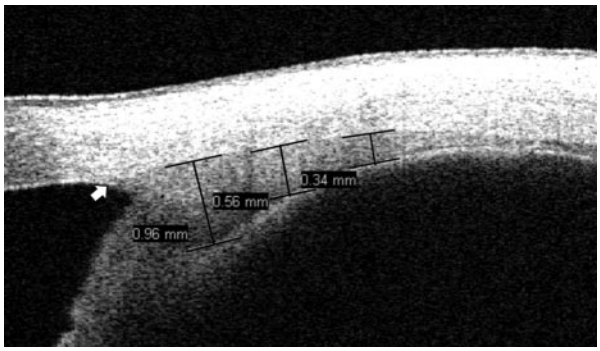

FIGURE 1. Representative image of the nasal ciliary body while the subject viewed an external fixation target. CBT1, -2, and -3 are 1, 2, and 3 mm posterior to the scleral spur (*arrow*), respectively.

design were approved by the Institutional Review Board at The Ohio State University.

Measurements

All measurements were made on the right eye only. All cycloplegic measurements were made with the following procedure. One drop of 0.5% proparacaine was instilled in the right eye followed by 2 drops of 1% tropicamide in each eye. The two drops of 1% tropicamide were instilled 5 minutes apart. Cycloplegic measurements were made 25 minutes after the last drop of tropicamide was instilled.

Refractive error was the mean spherical equivalent of five cycloplegic measurements taken with a binocular autorefractor/keratometer (WR-5100K; Grand Seiko Co., Ltd., Hiroshima, Japan). Axial length measurements were the mean of three measurements made with an optical biometer (IOLMaster; Carl Zeiss Meditec, Inc., Dublin, CA). Ciliary body thickness (CBT) measurements were made with an anterior segment OCT instrument (Visante; Carl Zeiss Meditec; Fig. 1). A subset of 38 children had CBT measurements made at a second study visit that was approximately 2 weeks after the initial study visit.

There are no previously published studies of CBT measurements made with images from an OCT (Visante; Carl Zeiss Meditec). Thus, a new protocol for obtaining the images of the ciliary body and measuring its dimensions was developed. Images were always obtained with the instrument in high-resolution corneal mode.

CBT Measurements

All ciliary body measurements were made under cycloplegic conditions. Initially, one image of the right eye was obtained while the child viewed the target inside the instrument and the eye was positioned to view the nasal ciliary body and sclera. A second image was obtained while the child viewed a fixation target outside of the instrument so that the ciliary body was imaged through the sclera. It became clear after testing a few children that the density of iris pigment in some made it impossible to obtain images of the ciliary body while the child looked directly into the instrument. Because myopia is the most prevalent in individuals of Asian descent who most often have dark-colored irises, restricting study entry to only subjects with light-colored irises did not seem appropriate. Therefore, after testing 25 children, all ciliary body images were obtained while the child viewed an external target. Only the images obtained when the children were viewing the external targets were used in statistical analyses.

Ciliary body images obtained during the study visits were processed with the OCT software (Visante; Carl Zeiss Meditec) to obtain thickness measurements at several locations along the length of the ciliary body. When the biometer is used to measure corneal thickness or anterior chamber depth, there are software adjustments that apply an appropriate refractive index to those structures within the image. In this study, the instrument was used to measure the ciliary body and the "appropriate" refractive index to apply to an image of the ciliary body is unknown. Thus, a refractive index of 1.0 was applied to the entire image before making measurements. Then, thickness measurements were obtained using the calipers supplied in the "analysis" mode of the system software. All measurements were made by one examiner (MDB), as described in the next section. This examiner was not masked when making CBT measurements.

All images for a given subject were viewed to identify precisely the location of the scleral spur in each subject. At times, this structure was clearly visible in one image for the subject, but more subtly visible in another image for the same subject. Viewing all images for a subject often allowed for more confident identification of the scleral spur. Once the scleral spur was identified in each image, one end of a caliper 1.00 mm in length was placed on the scleral spur. The other end of the caliper was placed along the border between the sclera and the ciliary body. This process was repeated for calipers that were 2.00 and 3.00 mm in length. The examiner was careful to place the scleral spur end of all calipers at the same location, overlying the scleral spur.

The software allows for up to seven calipers to be applied to an image, and it also allows the user to "hide" or "show" calipers overlying the image without deleting or moving them. Using this feature of the software, CBT measurements were then made 1.00 mm posterior to the scleral spur while the 2.00- and 3.00-mm calipers were hidden from view. The intraocular boundaries of the sclera and the external edge (scleral, nonvitreous) of the ciliary pigmented epithelium were identified in the images, and these structures served as the boundaries for the thickness measurements. The caliper used to measure the thickness at 1.00 mm (CBT1) posterior to the scleral spur was aligned so that it was perpendicular to the local curvature of the sclera, and then the other end was extended toward the ciliary pigmented epithelium. This process was then repeated at 2.00 mm (CBT2) and 3.00 mm (CBT3) posterior to the scleral spur. Thus, three thickness measurements were obtained, CBT1, -2, and -3 (Fig. 1).

Once this process was completed on all images for all subjects, they were then viewed a second time. All six calipers, three marking the relevant distances posterior to the scleral spur and the three calipers measuring the thickness of the ciliary body were hidden from view. The scleral spur was identified visually in the image and then each of the three calipers marking the distance from the scleral spur was made visible. The examiner confirmed that one end of these calipers was indeed marking the scleral spur. Minor adjustments were made if required. Next, each of the calipers measuring the thickness of the ciliary body was examined to make sure that the caliper was positioned 1.00, 2.00, or 3.00 mm posterior to the scleral spur, that it was aligned perpendicular to the local curvature of the sclera, and that it extended appropriately to the edge of the ciliary pigmented epithelium. Again, minor adjustments were made if required. Finally, each of the three measurements was recorded for the image in a computer spreadsheet (Excel; Microsoft, Redmond, WA). The biometry system software provides measurements in 10-μm increments.

A subset of 133 images was used to determine the repeatability of the examiner's identification of the scleral spur. Approximately half of these images were from subjects with myopic eyes and the other half were from subjects with nonmyopic eyes. The scleral spur was marked in each image, three different times. In commercial software (MatLab; MathWorks, Natick, MA), the x and y pixel coordinates of the position marked as the scleral spur were identified. Thus, the examiner's choice of the scleral spur location was determined independently three times, and the repeatability of that choice was then determined for each image.

Statistical Analyses

The relationship between CBT and refractive error and axial length was assessed using multilevel models[17] with CBT as an outcome and refractive error and axial length as predictors. Independent models were fitted for each predictor.

The process of model term selection was the same for each predictor. A control model of CBT was fitted by using age and sex as

TABLE 1. Demographic Characteristics of the Study Sample

Measurement	Mean	SD	Minimum	Maximum
Age (y)	11.79	2.31	8.17	15.14
Refractive error (D)	−1.13	2.26	−6.00	3.44
CBT (μm)				
CBT1	899.43	121.71	600.00	1112.50
CBT2	601.49	101.55	385.00	830.00
CBT3	326.27	69.85	130.00	470.00
Axial length (mm)	23.81	1.15	22.14	26.81

CBT1, 1 mm posterior to the scleral spur; CBT2, 2 mm posterior to the scleral spur; and CBT3, 3 mm posterior to the scleral spur.

control variables. The control model included all two-way interactions of the control predictors. None of these interactions were statistically significant ($\alpha = 0.05$), and they were removed from the model. After the control model was selected, a question predictor was added (refractive error or axial length), as well as all two-way interactions between the question predictor and control predictors. For both refractive error and axial length, none of the interactions with control predictors was statistically significant. Thus, these interaction terms were not included in the final model. The final models had the following form:

$$\mathrm{CBT}_{ijk} = \mu_j + \alpha_j \cdot \mathrm{QP}_i + \gamma_i + \tau \cdot \mathrm{age}_{ik} + \xi_i + \varepsilon_{ijk}$$

where, i indexed the subject, j the location of the thickness measurement (1, 2, or 3 mm behind the scleral spur), and k the within-subject CBT measurement, with up to four measurements of each location available for each subject. The model had two random components: ξ and ε. The ξ term captured the between-subject error and modeled the correlation among CBT measurements taken from the same subject. The ε term captured the within-subject error. The nonrandom model parameters included the intercept μ, α, γ, and τ. QP signifies the question predictor (either refractive error or axial length). The gender parameter was γ, with sex coded as an indicator (male, 0; female, 1). The intercept and α (the slope of the question predictor) were allowed to vary with the location of measurement. In the data, CBT and age were time variant, but refractive error was time invariant. All modeling was performed in commercial software (SAS ver. 9.1 using the MIXED procedure; SAS Institute, Cary, NC).

To assess the within-visit and between-visit repeatability of the CBT measurements, the method described by Bland and Altman[18] was used. The mean difference between the repeated measurements (i.e., the difference between two measurements taken at one visit or the difference between the two visits) characterizes the bias of the method. Whether the bias was statistically significant (different from 0) was assessed by constructing a 95% confidence interval for the bias estimate. The mean and the SD of differences were used to construct 95% limits of agreement (LoA; mean ± [1.96 · SD]). The LoA characterize the expected differences between repeated measurements. The coefficient of repeatability (1.96 · SD of the differences), an indicator of the amount of variation that can be attributed to measurement error, was also calculated.

RESULTS

The general characteristics of the study sample are displayed in Table 1. Children with a wide range of refractive errors were included. Almost all the children in the study were Caucasian (50/53); the other three subjects were African American. The CBT measurements were thickest, as one would expect, when the measurement was made closer to the scleral spur (CBT1, mean ± SD = 899.4 ± 121.7 μm) and smallest at the measurement point farthest from the scleral spur (CBT3, mean ± SD = 326.27 ± 69.85 μm). The three CBT measurements were correlated with one another. CBT1 correlated more strongly correlated CBT2 ($r = 0.48$, $P < 0.001$) than with CBT3 ($r = 0.38$, $P < 0.001$). The highest correlation was found between CBT2 and -3 ($r = 0.85$, $P < 0.001$). Table 2 displays the mean CBT at CBT1, -2, and -3 for the emmetropic subjects (spherical equivalent refractive errors, ≤2.00 D and > −0.75 D) and myopic subjects (spherical equivalent refractive error, ≤ −0.75 D). There were only two subjects who met the definition of hyperopia (spherical equivalent refractive error, >2.00 D), and so those subjects were not included in the table. Note that this sample had only two children who are hyperopic. The myopic subjects in the sample tended to be older ($r = -0.58$, $P < 0.001$), and so the multilevel models included age to account for this relationship.

Repeatability of CBT Measurements

For all comparisons of the within-visit measurements and the between-visit measurements (Table 3), no statistically significant bias in the measurement methods was found. The coefficient of repeatability for within-visit comparisons was 152.94 μm for CBT1, 179.95 μm for CBT2, and 131.24 μm for CBT3. For between-visit comparisons, the coefficient of repeatability was similar to that of the within-visit comparisons (CBT1 = 148.04 μm, CBT2 = 165.68 μm, and CBT3 = 110.90 μm).

When the scleral spur was identified three times in the same image ($n = 133$ images), the mean distance (± SD) of each of the three points from the mean location of the three points was 3.98 (± 2.89) pixels. The median distance was 3.35 pixels, and the range was 0.67 to 18.60 pixels. In these images, one pixel is equivalent to approximately 12.2 μm. Thus, the mean distance of the examiner's choice of the scleral spur from the mean of those three choices was approximately 48.6 μm.

CBT and Refractive Error

There was a statistically significant univariate correlation between refractive error and CBT2 ($r = -0.29$, $P = 0.03$) and CBT3 ($r = -0.38$, $P = 0.005$), but not CBT1 ($r = -0.016$, $P =$

TABLE 2. CBT Measurements by Refractive Error Status

	Emmetropia ($n = 25$)		Myopia ($n = 26$)	
CBT	Mean	SD	Mean	SD
CBT1	894.6	126.8	903.3	119.1
CBT2	573.9	100.4	629.7	99.8
CBT3	296.0	61.0	354.7	68.1

CBT measurements are as described in Table 1. Emmetropia, spherical equivalent refractive error ≤ 2.00 D and > −0.75 D; myopia, spherical equivalent refractive error ≤ −0.75 D

TABLE 3. Bias, or Mean Difference, and 95% LoA for the Within-Visit Comparisons and Between-Visit Comparisons of CBT Measurements

Measurement	Mean Difference	SD of the Differences	95% LoA
Within-visit comparisons			
CBT1	0.67	78.03	−152.27,+153.61
CBT2	7.00	91.81	−172.95,+186.95
CBT3	13.00	66.96	−118.24,+144.24
Between-visit comparisons			
CBT1	−6.58	75.53	−154.62,+141.46
CBT2	−8.16	84.53	−173.83,+157.52
CBT3	6.58	56.58	−104.32,+117.48

Thickness data are expressed in micrometers. CBT locations are as in Table 1.

0.91). The multilevel model was fitted using 435 measures from 53 children (Table 4). Because measurements closer to the scleral spur were thicker, there was a statistically significant effect of the location of the measurement in the model in Table 4. There was a statistically significant interaction between the location of the CBT measurement and refractive error, with a significant, negative association between refractive error and the measurements CBT2 and -3. No significant relationship was found for CBT1 and refractive error. Figure 2 demonstrates this interaction between location and refractive error through model projections of the relationship between CBT and refractive error; one can observe that the slope of the regression line for CBT1 is relatively flat compared to the steeper negative slope of the regression lines for CBT2 and -3.

CBT and Axial Length

There was a statistically significant univariate correlation between axial length and CBT2 ($r = -0.40$, $P = 0.003$) and CBT3 ($r = -0.51$, $P < 0.001$), but not between axial length and CBT1 ($r = 0.11$, $P = 0.46$). The model for CBT and axial length was fitted by using 417 measures from 51 children (Table 5). There was a significant interaction between the location of the CBT measurement and axial length, as depicted in Figure 3. Eyes with a longer axial length were found to have a thicker ciliary body. The strongest association between CBT and axial length was found for CBT2, followed by CBT3 and then CBT1.

DISCUSSION

Measurement of the ciliary body dimensions is not a routine practice in either clinical vision care or clinical vision research. In fact, this study may be the largest in vivo report of ciliary body dimensions in a pediatric sample. Because advances in biological imaging provided the means to collect these data, we were able to determine whether the ciliary body was thicker in myopic children.

The thickness of the ciliary body was measured at three locations. Thickness at the two most posterior locations (CBT2 and CBT3) correlated negatively with refractive error and positively correlated with axial length. Oliveira et al.[15] found very similar results in adults, with the strongest associations found between CBT2 and refractive error and axial length. The refractive error correlation coefficients in Oliveira et al. were higher than those found in our study (CBT2: $r = -0.64$ in adults vs. -0.29 in children). A possible explanation for this difference in the strength of the association is that this was a cross-sectional sample of children who had not yet reached their final, adult refractive error status (i.e., some of the emmetropic children may still become myopic). If one examines the closed circles in Figure 2, it is apparent that some of the emmetropic data points are associated with CBT measurements that are similar to those in the myopic eyes. Are the emmetropic children with thick ciliary bodies in this cross-sectional sample prone to developing myopia in the future? The normal variation in CBT in emmetropic eyes is still unknown. The full meaning of these associations among CBT, refractive error, and axial length is also uncertain.

Where does this new association fit within the body of knowledge that describes the etiology of myopia? Is there something about the genetic or environmental factors that cause myopia that also leads to a thicker ciliary body? Can the process that makes the ciliary body thicker and/or the biomechanical effects of the thicker ciliary body itself lead to elongation of the globe? What portion of the ciliary body is thickened: the muscle, the stromal tissue, or both? Why is the tissue thickened? The answer to these questions will not be found in

TABLE 4. Multilevel Linear Regression Model for CBT and Refractive Error in Children.

Predictor	*P*	Location	Parameter Estimate
Intercept			314.87
Location of the CBT measurement (μm)	<0.001	CBT1	601.43
		CBT2	275.48
		CBT3	0.00
Refractive error (D)	0.10		−14.68
Age (relative to 8 years)	0.63		−2.89
Sex (female, 1; male, 0)	0.88		3.64
Location of CBT measurement/Refractive error interaction	<0.001	CBT1	15.26
		CBT2	−1.75
		CBT3	0.00

CBT locations are as in Table 1.

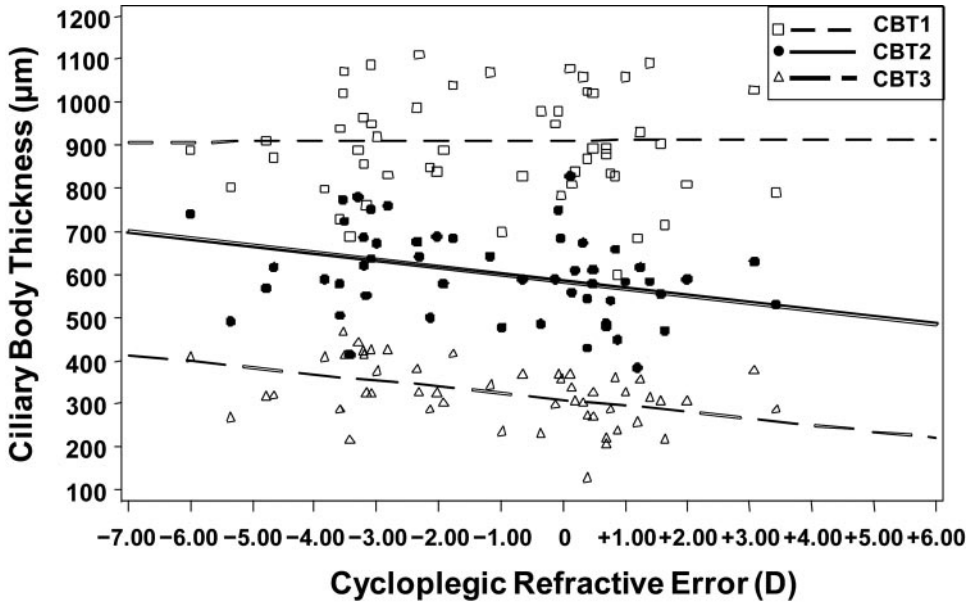

FIGURE 2. Model projections of the relationship between CBT and refractive error. There was a significant interaction between the location of the CBT measurement 1 (CBT1), 2 (CBT2), or 3 (CBT3) mm posterior to the scleral spur) and refractive error ($P < 0.001$). The thickness at CBT2 and -3 were associated with refractive error, but CBT1 was not associated with refractive error.

the data presented herein; much further investigation is needed.

Of course, it is possible that this new association has little relevance to myopia. Still, one might begin to speculate on the topic by considering what has been established in the field of myopia research. As discussed in the introduction of this report, the fact that the myopic eye is generally more prolate than the emmetropic eye is supported by several different studies in which different types of technology were used to measure the shape of the globe (ocular biometry and MRI) and different study designs (both cross-sectional and longitudinal).[1–3] The etiology of myopia, or the process that leads to this more prolate globe shape, is the element that is uncertain.

The prevailing theory regarding the etiology of juvenile-onset myopia is the hyperopic defocus model (Fig. 4A), and it is supported by a substantial body of work in animal models.[12–14,19–24] There are also human clinical studies demonstrating that children with myopia accommodate less accurately than children who do not have myopia.[25–27] If the hyperopic defocus model is an accurate depiction of the etiology of myopia, how would the enlarged ciliary body fit into this model? In the case of differential growth of the axial and transverse regions of the globe,[3] it is difficult to imagine how growth in the posterior pole alone would lead to a thicker ciliary body. In the scenario outlined in Figure 4A, an abnormality of the ciliary muscle could be the source of accommodative lag (the "?" in Fig. 4A), leading to retinal defocus and axial elongation.

The causal relationship of accommodative dysfunction and myopia, the second arrow in Figure 4A, is still questioned; the debate continues because there are conflicting reports on the temporal relationship between accommodative lag and the onset of myopia. Two smaller studies have found reduced accommodation before myopia onset,[28,29] while the larger, ethnically diverse CLEERE Study reports higher amounts of accommodative lag only after myopia onset.[27] Thus, the existing longitudinal data on myopia's development in humans do not appear to unequivocally support the hyperopic defocus model (Fig. 4A).

In a 1995 publication, Gwiazda et al.[25] state that others have "questioned whether this accommodative abnormality was a cause or effect of myopia. Yet another possibility is that a common factor, as yet unidentified, accounts for both." As stated earlier, CLEERE Study investigators have proposed that the crystalline lens could lead to a prolate globe shape through an internal, equatorial growth restriction.[1] While initial investigations into an association between crystalline lens tension and refractive error showed no relationship between the two (Bailey MD, et al. *IOVS.* 2008;49:ARVO E-Abstract 3579 and manuscript in preparation), a thickened ciliary muscle may also serve as an internal equatorial growth restriction, and the "yet unidentified" factor that would lead to both accommodative lag and axial elongation in myopia (Fig. 4B).

The regions of the ciliary body that showed the strongest relationships with refractive error, axial length, and a more

TABLE 5. Multilevel Linear Regression Model for CBT and Axial Length in Children

Predictor	*P*	Location	Parameter Estimate
Intercept			261.52
Location of the CBT measurement (µm)	<0.001	CBT1	628.57
		CBT2	265.52
		CBT3	0.00
Axial length (relative to 22.0 mm)	0.001		48.25
Age (relative to 8 y)	0.07		−11.60
Sex (female, 1; male, 0)	0.24		27.46
Location of CBT measurement/axial length interaction	<0.001	CBT1	−25.07
		CBT2	7.11
		CBT3	0.00

CBT locations are as in Table 1.

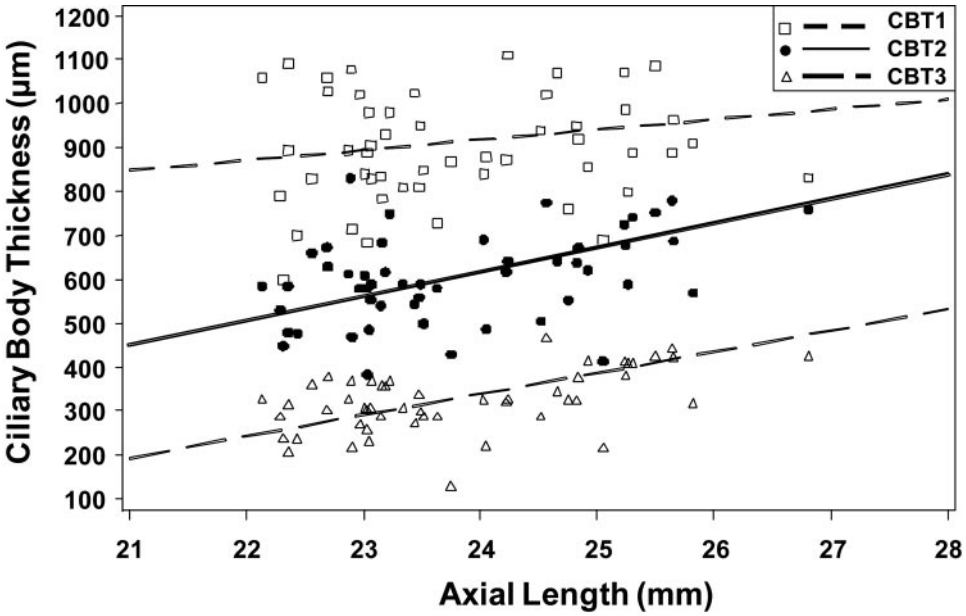

FIGURE 3. Model projections of the relationship between CBT and axial length. There was a significant interaction between the location of CBT measurement, 1 (CBT1), 2 (CBT2), or 3 (CBT3) mm posterior to the scleral spur, and refractive error ($P < 0.001$). CBT was associated with refractive error at all three measurement locations, but the association was stronger for CBT2 and -3 than for CBT1.

prolate globe shape, were the areas of the ciliary body that should primarily consist of ciliary muscle tissue, CBT2 and -3. Conversely, CBT1 would consist of a higher proportion of stromal tissue relative to CBT2 and CBT3. No association between CBT1 and refractive error was found, and weaker associations were found for CBT1 and axial length. Either the stromal tissue varies randomly in thickness at CBT1 and obscures associations between CBT and refractive error, or the quality of the image at this location leads to random error (discussed further later). Nonetheless, for the sake of argument, if one assumes the thickening of the ciliary body is due to a thickening of the ciliary muscle, an explanation of ciliary muscle hypertrophy could be considered. In hypertrophy of smooth muscle organs, the smooth muscle cells become enlarged and contract poorly.[30] A thickened, poorly contracting ciliary muscle could explain the accommodative abnormalities that are a hallmark of juvenile myopia.

The mechanism by which a thickened ciliary muscle would lead to both accommodative abnormalities and axial elongation *independently* is not readily apparent. A thickened ciliary muscle does not seem to be a simple consequence of an elongated eye. Based on the choroidal expansion models of van Alphen,[16] one would expect the enlarged myopic globe to have a *thinner* ciliary muscle. Perhaps the muscle thins initially, as van Alphen predicted, and then the ciliary body thickens as a later response in the process of myopia's development. Alternatively, biochemical processes may underlie both muscle thickening and axial elongation simultaneously. The increased activation of MMP-2[31] that is known to lead to scleral remodeling in the tree shrew model of myopia is also expressed by ciliary muscle cells.[32] Increased activation of MMP-2 in the ciliary muscle, however, leads to a thickening of the ciliary body at the identical locations noted in the present study, CBT2 and -3, with the use of prostaglandin analogues.[33] A longitudinal study is necessary, to determine both the temporal relationship between ciliary body thickening and axial elongation and to determine whether van Alphen's prediction of ciliary muscle thinning occurs at any point in the process. Thus, there are several reasons for continuing to investigate the relationships depicted in Figure 4A. These data are also cause for investigat-

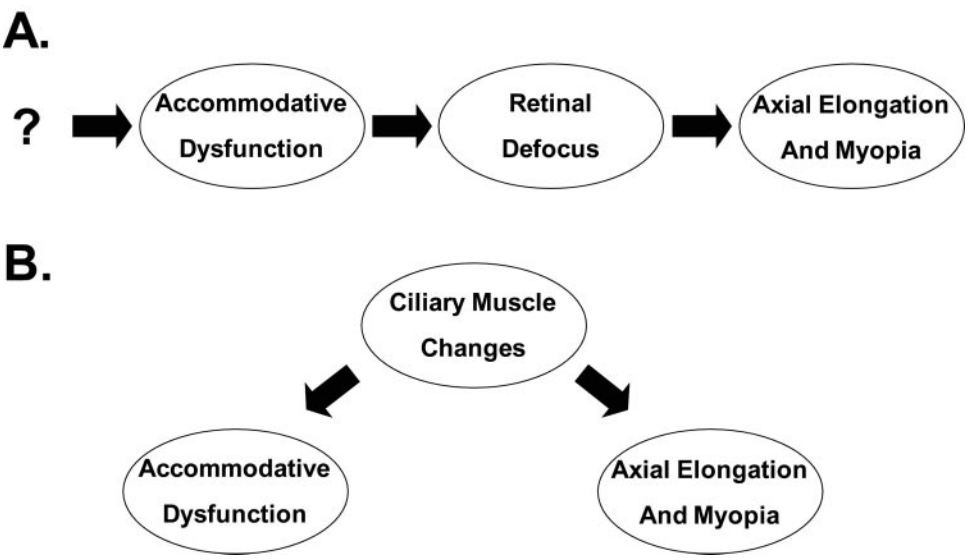

FIGURE 4. (**A**) In the hyperopic defocus model, the prevailing hypothesis of myopia's development, the cause of accommodative dysfunction is unknown. (**B**) In the equatorial growth restriction model of myopia's development, the initiating event is hypertrophy of the ciliary muscle; which also causes accommodative dysfunction.

ing whether any changes occur in the ciliary body during experimentally induced myopia. The ciliary body appears to be thicker in human myopia. Is it also thicker in animal models of myopia?

It was impossible to determine with the OCT (Visante; Carl Zeiss Meditec) if the ciliary muscle is longer in myopic eyes than in nonmyopic eyes; the posterior attachment of the zonules was not visible. In globe expansion studies, van Alphen[16] found elongation of the ciliary muscle. If a longer ciliary muscle leads to elongation of the uvea, it could explain the axial elongation observed in myopia. In addition, hypertrophy in other smooth muscle tissues can lead to a process of fibrosis and excessive collagen deposition.[30] In the ciliary muscle, collagen fibers are known to "interweave with each other to form large and compact bundles [running] in a circular direction as the circular muscle."[34] If hypertrophy of the ciliary muscle results in excessive deposition of collagen running in a circular orientation, the hypertrophic ciliary muscle may serve as an equatorial growth restriction, leading to uncompensated axial elongation.[1] Both of these possibilities are purely speculative and need further investigation.

When considering the implications of the findings of this study, its limitations should also be considered. The most important limitation is that the data were drawn from a clinical sample of convenience and may not be representative of the myopic condition as a whole. Collection of these data should be repeated in a nonclinical sample, in which myopic subjects at all stages of myopia progression can be measured.

One additional limitation of the present study was the repeatability of the CBT measurements and the minor variability in the examiner's ability to choose the identical pixel coordinates for the scleral spur on repeated attempts. The SD for measurements of CBT at CBT2 for all subjects was 102 μm, but the between-visits coefficient of repeatability for CBT2 was similar in magnitude, 166 μm. In other words, these measurements were not optimally precise, as the variability across subjects was similar to that of the variability associated with repeated measurements. Determination of the ciliary pigmented epithelium boundary for the CBT1 thickness location was challenging because it was not very distinct in the image (Fig. 1). (Coincidentally, at the time of writing this report, Carl Zeiss Meditec released a software update for the Visante, version 2.0, that should assist in improving the quality of the images obtained. According to the manufacturer, Version 2.0 is expected to provide enhanced image quality "with image averaging and registration to provide even greater visual detail in anterior segment and corneal images.")

An automated image analysis method using these new images is in development by the authors. In this program (MatLab; The MathWorks), a mean location for several selections of the scleral spur and an algorithm-derived measurement scheme is used to measure the dimensions of the ciliary body. Still, it is expected that researchers will have to use a mean of several measurements in research involving the ciliary body. There are no distinct landmarks for the alignment of the measurements, and minor rotational changes in eye position can affect the plane in which the image is acquired. An automated measurement method, however, should make the process of measuring the dimensions in multiple images for each subject more feasible.

In summary, this study documents the existence of a thicker ciliary body in children who are myopic compared to children who are not myopic. Further investigation is necessary to determine the meaning of this association, if any. Improvements in the precision of the CBT measurements made with the OCT (Visante; Carl Zeiss Meditec) are also needed.

References

1. Mutti DO, Hayes JR, Mitchell, et al. Refractive error, axial length, and relative peripheral refractive error before and after the onset of myopia. *Invest Ophthalmol Vis Sci*. 2007;48(6):2510–2519.
2. Atchison DA, Jones CE, Schmid KL, et al. Eye shape in emmetropia and myopia. *Invest Ophthalmol Vis Sci*. 2004;45(10):3380–3386.
3. Logan NS, Gilmartin B, Wildsoet CF, Dunne MC. Posterior retinal contour in adult human anisomyopia. *Invest Ophthalmol Vis Sci*. 2004;45(7):2152–2162.
4. Ferree CE, Rand G, Hardy C. Refraction for the peripheral field of vision. *Arch Ophthalmol*. 1931;5:717–731.
5. Rempt F, Hoogerheide J, Hoogenboom WP. Peripheral retinoscopy and the skiagram. *Ophthalmologica*. 1971;162(1):1–10.
6. Millodot M. Effect of ametropia on peripheral refraction. *Am J Optom Physiol Opt*. 1981;58(9):691–695.
7. Charman WN, Jennings JA. Ametropia and peripheral refraction. *Am J Optom Physiol Opt*. 1982;59(11):922–923.
8. Hoogerheide J, Rempt F, Hoogenboom WP. Acquired myopia in young pilots. *Ophthalmologica*. 1971;163(4):209–215.
9. Smith EL 3rd, Kee CS, Ramamirtham R, Qiao-Grider Y, Hung LF. Peripheral vision can influence eye growth and refractive development in infant monkeys. *Invest Ophthalmol Vis Sci*. 2005; 46(11):3965–3972.
10. Smith EL 3rd, Ramamirtham R, Qiao-Grider Y, et al. Effects of foveal ablation on emmetropization and form-deprivation myopia. *Invest Ophthalmol Vis Sci.* 2007;48(9):3914–3922.
11. Schaeffel F, Glasser A, Howland HC. Accommodation, refractive error and eye growth in chickens. *Vision Res*. 1988;28(5):639–657.
12. Irving EL, Sivak JG, Callender MG. Refractive plasticity of the developing chick eye. *Ophthalmic Physiol Opt*. 1992;12(4):448–456.
13. Wildsoet C, Wallman J. Choroidal and scleral mechanisms of compensation for spectacle lenses in chicks. *Vision Res*. 1995;35(9): 1175–1194.
14. Smith EL 3rd, Hung LF. The role of optical defocus in regulating refractive development in infant monkeys. *Vision Res*. 1999;39(8): 1415–1435.
15. Oliveira C, Tello C, Liebmann JM, Ritch R. Ciliary body thickness increases with increasing axial myopia. *Am J Ophthalmol*. 2005; 140(2):324–325.
16. van Alphen GW. Choroidal stress and emmetropization. *Vision Res*. 1986;26(5):723–734.
17. Snijders TAB, Bosker RJ. *Multilevel Analysis*: *an Introduction to Basic and Advanced Multilevel Modeling.* Thousand Oaks, CA: Sage Publications; 1999:viii:266.
18. Bland JM, Altman DG. Statistical methods for assessing agreement between two methods of clinical measurement. *Lancet*. 1986; 1(8476):307–310.
19. Graham B, Judge SJ. The effects of spectacle wear in infancy on eye growth and refractive error in the marmoset (Callithrix jacchus). *Vision Res*. 1999;39(2):189–206.
20. Schaeffel F, Troilo D, Wallman J, Howland HC. Developing eyes that lack accommodation grow to compensate for imposed defocus. *Vis Neurosci*. 1990;4(2):177–183.
21. Shen W, Vijayan M, Sivak JG. Inducing form-deprivation myopia in fish. *Invest Ophthalmol Vis Sci*. 2005;46(5):1797–1803.
22. Siegwart JT Jr, Norton TT. The time course of changes in mRNA levels in tree shrew sclera during induced myopia and recovery. *Invest Ophthalmol Vis Sci*. 2002;43(7):2067–2075.
23. Wallman J, Turkel J, Trachtman J. Extreme myopia produced by modest change in early visual experience. *Science*. 1978; 201(4362):1249–1251.
24. Wallman J, Wildsoet C, Xu A, et al. Moving the retina: choroidal modulation of refractive state. *Vision Res*. 1995;35(1):37–50.
25. Gwiazda J, Thorn F, Bauer J, Held R. Myopic children show insufficient accommodative response to blur. *Invest Ophthalmol Vis Sci*. 1993;34(3):690–694.
26. Gwiazda J, Bauer J, Thorn F, Held R. A dynamic relationship between myopia and blur-driven accommodation in school-aged children. *Vision Res*. 1995;35(9):1299–1304.
27. Mutti DO, Mitchell GL, Hayes JR, et al. Accommodative lag before and after the onset of myopia. *Invest Ophthalmol Vis Sci*. 2006; 47(3):837–846.

28. Goss DA. Clinical accommodation and heterophoria findings preceding juvenile onset of myopia. *Optom Vis Sci*. 1991;68(2):110–116.
29. Gwiazda J, Thorn F, Held R. Accommodation, accommodative convergence, and response AC/A ratios before and at the onset of myopia in children. *Optom Vis Sci*. 2005;82(4):273–278.
30. Seidel CL, Weisbrodt NW. *Hypertrophic Response in Smooth Muscle*. Boca Raton, FL: CRC Press; 1987:199.
31. Guggenheim JA, McBrien NA. Form-deprivation myopia induces activation of scleral matrix metalloproteinase-2 in tree shrew. *Invest Ophthalmol Vis Sci*. 1996;37(7):1380–1395.
32. Weinreb RN, Kashiwagi K, Kashiwagi F, Tsukahara S, Lindsey JD. Prostaglandins increase matrix metalloproteinase release from human ciliary smooth muscle cells. *Invest Ophthalmol Vis Sci*. 1997; 38(13):2772–2780.
33. Marchini G, Ghilotti G, Bonadimani M, Babighian S. Effects of 0.005% latanoprost on ocular anterior structures and ciliary body thickness. *J Glaucoma*. 2003;12(4):295–300.
34. Wang YD, Chen HB, Jin M, et al. Three-dimensional arrangement of collagen fibrils in human ciliary body. *Ophthalmic Res*. 1999; 31(5):378–386.